

Provided for non-commercial research and education use.  
Not for reproduction, distribution or commercial use.



This article appeared in a journal published by Elsevier. The attached copy is furnished to the author for internal non-commercial research and education use, including for instruction at the authors institution and sharing with colleagues.

Other uses, including reproduction and distribution, or selling or licensing copies, or posting to personal, institutional or third party websites are prohibited.

In most cases authors are permitted to post their version of the article (e.g. in Word or Tex form) to their personal website or institutional repository. Authors requiring further information regarding Elsevier's archiving and manuscript policies are encouraged to visit:

<http://www.elsevier.com/authorsrights>



Contents lists available at ScienceDirect

## Ultrasonics

journal homepage: [www.elsevier.com/locate/ultras](http://www.elsevier.com/locate/ultras)

# Air-coupled detection of nonlinear Rayleigh surface waves to assess material nonlinearity



Sebastian Thiele<sup>a</sup>, Jin-Yeon Kim<sup>a</sup>, Jianmin Qu<sup>b</sup>, Laurence J. Jacobs<sup>a,c,\*</sup>

<sup>a</sup> School of Civil and Environmental Engineering, Georgia Institute of Technology, 30332 Atlanta, GA, United States

<sup>b</sup> Department of Civil and Environmental Engineering, Northwestern University, 60208 Evanston, IL, United States

<sup>c</sup> G.W. Woodruff School of Mechanical Engineering, Georgia Institute of Technology, 30332 Atlanta, GA, United States

## ARTICLE INFO

### Article history:

Received 30 October 2013

Received in revised form 9 April 2014

Accepted 20 April 2014

Available online 2 May 2014

### Keywords:

Nonlinear ultrasound  
Rayleigh surface waves  
Air-coupled transducer

## ABSTRACT

This research presents a new technique for nonlinear Rayleigh surface wave measurements that uses a non-contact, air-coupled ultrasonic transducer; this receiver is less dependent on surface conditions than laser-based detection, and is much more accurate and efficient than detection with a contact wedge transducer. A viable experimental setup is presented that enables the robust, non-contact measurement of nonlinear Rayleigh surface waves over a range of propagation distances. The relative nonlinearity parameter is obtained as the slope of the normalized second harmonic amplitudes plotted versus propagation distance. This experimental setup is then used to assess the relative nonlinearity parameters of two aluminum alloy specimens (Al 2024-T351 and Al 7075-T651). These results demonstrate the effectiveness of the proposed technique – the average standard deviation of the normalized second harmonic amplitudes, measured at locations along the propagation path, is below 2%. Experimental validation is provided by a comparison of the ratio of the measured nonlinearity parameters of these specimens with ratios from the absolute nonlinearity parameters for the same materials measured by capacitive detection of nonlinear longitudinal waves.

© 2014 Elsevier B.V. All rights reserved.

## 1. Introduction

An ultrasonic wave propagating in an elastic material generates higher harmonics through its interaction with various sources of nonlinearity in a material. The non-dimensional acoustic nonlinearity parameter,  $\beta$  relates the amplitudes of the fundamental and second harmonic waves, providing information on the microstructure of a material. The acoustic nonlinearity parameter has proven to be sensitive to certain microstructural changes such as those due to precipitation [1], creep [2], fatigue [3], thermal [4] or radiation damage [5], and is therefore a powerful indicator of the material state.

The most commonly used nonlinear wave technique uses through-transmitted longitudinal waves, which is often difficult to apply in the field since access to both sides of the specimen is required. Rayleigh surface waves have the advantage, as compared to longitudinal waves, that they require access to only one side of a component. In addition, diffraction and attenuation effects are

smaller, and Rayleigh surface waves travel a long distance without a significant loss of acoustic energy. Most importantly, it is possible to effectively isolate the material contribution in the measured second harmonic component by varying the propagation distance; here the unwanted nonlinearity from the measurement system will remain constant (or decrease), while the material nonlinearity will increase with increasing propagation distance. These features make Rayleigh waves an efficient method for measuring the material nonlinearity and thus this technique can be used for the non-destructive, in situ surveillance of complex components.

Experimental setups that employ wedge transducers for both transmission and detection have been used [6,7,4] to perform nonlinear Rayleigh surface wave measurements. However, these have shown to be time consuming and can suffer from large variations due to the inconsistent contact conditions at the wedge-specimen interface. These circumstances lead to opportunities for measurement improvements, and non-contact methods can potentially make nonlinear Rayleigh wave measurements more flexible, less time consuming, and more accurate. A Michelson interferometer detection setup to perform nonlinear Rayleigh wave measurements was used by Hurley and Fortunko [8], which had the advantage of having a broadband response and simple calibration, and made absolute displacement measurements. Herrmann et al. [9]

\* Corresponding author at: School of Civil and Environmental Engineering, Georgia Institute of Technology, 30332 Atlanta, GA, United States. Tel.: +1 404 894 2344; fax: +1 404 8940168.

E-mail address: [laurence.jacobs@ce.gatech.edu](mailto:laurence.jacobs@ce.gatech.edu) (L.J. Jacobs).

used a heterodyne laser interferometer detection setup for nonlinear Rayleigh wave measurements. However, the laser based detection of ultrasonic waves suffers from variations in optical reflectivity of the specimen surface and is only feasible for specimens with highly reflective surfaces. A recent study of Cobb et al. [10] makes use of electromagnetic acoustic transducers (EMATs) to perform fully non-contact nonlinear Rayleigh wave measurements, but they did not achieve the desired consistency.

The objective of the current research is to explore the feasibility of a non-contact, air-coupled detection technique to assess the acoustic nonlinearity parameter using Rayleigh surface waves. In principle, the assessment of the absolute acoustic nonlinearity parameter,  $\beta$  is possible using Rayleigh surface waves by making a series of electroacoustic calibrations and diffraction corrections. However, for the purpose of demonstrating the efficiency of using air-coupled detection, this study considers a relative acoustic nonlinearity parameter  $\beta'$  and compares the relative nonlinearities between two different specimens when all other experimental parameters are kept constant.

## 2. Theoretical Background

Consider a Rayleigh wave propagating in the  $x$  direction, where the  $z$  direction is pointing out of the half-space. The displacement field  $u_i(\omega_0)$  of the fundamental wave is given by

$$u_x(\omega_0) = A_1 \left( e^{b_1 z} - \frac{2b_1 b_2}{k_R^2 + b_2^2} e^{b_2 z} \right) \exp[ik_R(x - c_R t)], \quad (1a)$$

$$u_z(\omega_0) = iA_1 \frac{b_1}{k_R} \left( e^{b_1 z} - \frac{2k_R^2}{k_R^2 + b_2^2} e^{b_2 z} \right) \exp[ik_R(x - c_R t)], \quad (1b)$$

where  $b_1^2 = k_R^2 - k_L^2$  and  $b_2^2 = k_R^2 - k_T^2$ . Note that  $k_R$ ,  $k_L$ , and  $k_T$  denote the wavenumber of the Rayleigh surface wave, the longitudinal wave and the shear wave in the material.

As shown by Herrmann et al. [9], the displacement field  $u_i(2\omega_0)$  of the second harmonic Rayleigh surface wave can be written for a material with weak quadratic nonlinearity at sufficiently large distances as

$$u_x(2\omega_0) \approx A_2 \left( e^{2b_1 z} - \frac{2b_1 b_2}{k_R^2 + b_2^2} e^{2b_2 z} \right) \exp[i2k_R(x - c_R t)], \quad (2a)$$

$$u_z(2\omega_0) \approx iA_2 \frac{b_1}{k_R} \left( e^{2b_1 z} - \frac{2k_R^2}{k_R^2 + b_2^2} e^{2b_2 z} \right) \exp[i2k_R(x - c_R t)]. \quad (2b)$$

Herrmann et al. [9] has derived the acoustic nonlinearity parameter in terms of the vertical displacements of the fundamental and second harmonic wave component at the surface  $u_z(z=0) = \bar{u}_z$ , yielding

$$\beta = \frac{\bar{u}_z(2\omega_0)}{\bar{u}_z^2(\omega_0)x} \frac{i8b_1}{k_L^2 k_R} \left( 1 - \frac{2k_R^2}{k_R^2 + b_2^2} \right), \quad (3)$$

where one can clearly recognize the proportionality

$$\beta \propto \frac{\bar{u}_z(2\omega_0)}{\bar{u}_z^2(\omega_0)x}, \quad (4)$$

which will be used in the subsequent applications.

Since the air-coupled receiver detects the longitudinal wave that is produced by the surface motion of the Rayleigh wave, it is necessary to relate the amplitude of the out-of-plane displacement component,  $u_z(\omega, x, y)$  of the Rayleigh wave to the displacement,  $u_i^{(L)}(\omega)$  of the leaked longitudinal wave into the adjacent fluid. The continuity of out-of-plane displacement at the solid/air interface has to hold; then the  $x$  and  $z$  displacement components of the longitudinal wave in air can be written as [11]

$$|u_x^{(L)}(\omega)| = \left( \frac{k_R^2(\omega)}{k_{air}^2(\omega) - k_R^2(\omega)} \right)^{1/2} |\bar{u}_z(\omega)|, \quad (5a)$$

$$|u_z^{(L)}(\omega)| = |\bar{u}_z(\omega)|. \quad (5b)$$

The angle  $\Theta_R$  with respect to the surface normal (see Fig. 1) at which the longitudinal wave propagates in air can be calculated as

$$\Theta_R = \arcsin \frac{|u_x^{(L)}(\omega)|}{\left( |u_x^{(L)}(\omega)|^2 + |u_z^{(L)}(\omega)|^2 \right)^{1/2}}, \quad (6)$$

$$= \arcsin \left( \frac{c_{air}}{c_R} \right), \quad (7)$$

which is consistent with the calculation based on Snell's law,  $c_{air}$  being the longitudinal wave speed in air and  $c_R$  the velocity of Rayleigh surface in the specimen. By combining Eqs. (5a) and (5b), one can calculate the amplitude of the out-of-plane displacement of the surface wave from the measured amplitude of the leaked longitudinal wave, yielding

$$\bar{u}_z(\omega) = u^{(L)}(\omega) \left( 1 + \frac{k_R^2(\omega)}{k_{air}^2(\omega) - k_R^2(\omega)} \right)^{-1/2}. \quad (8)$$

Note that the lossless plane wave assumption for the Rayleigh wave shown in Eq. (3) leads to a definition of the acoustic nonlinearity parameter that neglects diffraction and attenuation effects in the actual experiments. However, the diffraction effect in Rayleigh waves is much smaller than that in three dimensional bulk waves. It can be shown for a 2.1 MHz fundamental wave component of a Rayleigh surface wave source with a Gaussian profile as discussed in Shull et al. [12], that the change in amplitude obtained by integrating over the transducer diameter of the receiving transducer for propagation distances between 30 mm and 78 mm decreases by only about 8%, if the diameter of the source and receivers are chosen to be 12.5 mm, and the attenuation of the solid is assumed to be 1 Np/m. This small change (–8%) in Rayleigh wave amplitude over the relevant propagation distances, obtained using the experimental parameters taken from the subsequent measurements (and assuming a Gaussian line source), justifies that the plane wave assumption is reasonable to apply for the evaluation of the experimental data in this research. Moreover, it has been shown experimentally and numerically that the ratio in Eq. (3) for a relatively short propagation distance is very close to linear.

## 3. Nonlinear Rayleigh wave measurement

### 3.1. Experimental setup using air-coupled receiver

A function generator is used (see Fig. 1) to obtain a sinusoidal signal at the excitation frequency of 2.1 MHz with a peak to peak

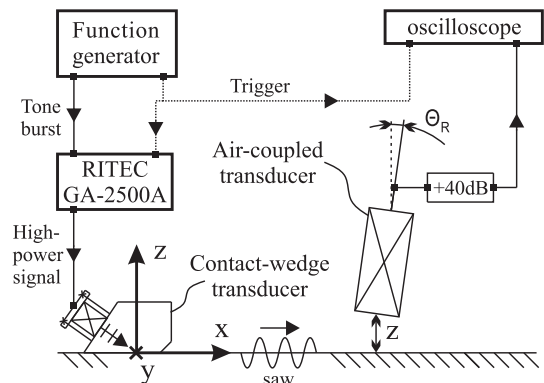


Fig. 1. Experimental setup using non-contact air-coupled receiver.

voltage of 800 mV. The source signal consists of 20 cycles, and provides a sufficiently long steady-state portion, which is important for the subsequent signal processing. The internal trigger of the function generator is used to synchronize the source with the RITEC amplifier and the oscilloscope. The desired high-voltage excitation signal for the generating transducer is obtained by amplifying the output signal of the function generator with a high power amplifier (RITEC GA-2500A). A high excitation signal is desirable to introduce waves with high enough acoustic energy to ensure a good signal-to-noise ratio (SNR) for the second harmonic component at the receiver. This type of amplifier provides a very clean output signal, and only introduces a very small amount of inherent nonlinearity.

The half-inch diameter narrow band piezoelectric contact transducer (Panametrics V-type) with a nominal center frequency of 2.25 MHz used for generation introduces a longitudinal wave in an acrylic wedge to excite a Rayleigh surface wave in the specimen. The frequency response of this transducer is shown in Fig. 2(a).

An acoustic coupling between the wedge and the sample is achieved with light lubrication oil, and the same oil also ensures acoustic coupling between the transducer and the wedge. The center frequency of the air-coupled receiver needs to be tuned around the frequency of the second harmonic wave to get the highest sensitivity at that frequency. An air-coupled transducer (Ultran NCT4-D13) with a nominal center frequency of 4 MHz is used in this research for detection. The air-coupled receiver detects the ultrasonic longitudinal wave which is leaked from the Rayleigh surface wave in the specimen. The actual center frequency of this transducer is at 3.9 MHz (Fig. 2(b)) and has an active area with a diameter of 12.5 mm.

The lift off distance  $z_0$  (Fig. 1) between the specimen and the midpoint of the active area of the air-coupled transducer is chosen as small as possible in the experimental setup to reduce attenuation and diffraction effects of the leaked ultrasonic waves in the air. It is limited to a minimum of 3.5 mm by the geometry of the air-coupled transducer and the radiation angle  $\Theta_R$ . The output signal at a lift off distance of  $z_0 = 3.5$  mm of the air-coupled transducer has about 2.5 mV peak-to-peak voltage when the Rayleigh surface wave is generated by a wedge transducer. The signal is amplified to obtain a sufficiently high SNR before recording it with the oscilloscope. The receiver part of a Panametrics 5072PR pulser-receiver is used to amplify the signal by 40 dB resulting in a peak-to-peak voltage of about 250 mV. The linearity of this preamplifier has been ensured in a previous experiment. The electrical output signal of the Panametrics 5072PR pulser-receiver is recorded by

an oscilloscope with a sampling rate of 250 MS/s and further averaged over 256 signals resulting in a SNR of 54 dB. Typical 256-times averaged time-domain signals are shown in Fig. 3 which demonstrate the stability of the entire measurement setup. The contributions of the first and second harmonic wave, which are depicted in Fig. 4 are obtained by performing a Fast Fourier transformation on the steady state portion of the time domain signal.

### 3.2. Experimental procedure

The electrical systems used to both excite and detect the propagating nonlinear Rayleigh waves are a potential source of nonlinearity, especially the high power amplifier and the exciting piezoelectric transducer, which can introduce spurious higher harmonic components. The amount of extraneous second harmonic component introduced by the high power amplifier, the exciting transducer and the coupling increases with increasing excitation voltage. One can therefore conclude that a measurement of the material nonlinearity parameter, using an increasing input voltage to excite Rayleigh waves with different amplitudes is only valid as long as the transducer and system nonlinearity are negligible, when compared to the second harmonic generated by the material nonlinearity. This is why the measurement technique with varying the Rayleigh wave propagation distance is useful to assess the acoustic nonlinearity parameter; the second harmonic component generated due to the system nonlinearity will remain constant (or decrease) with propagation distance, while the nonlinear material contribution should increase with increasing propagation distance.

The normalized second harmonic amplitude, i.e. the ratio of the second harmonic amplitude and fundamental amplitude squared (as shown in Eq. (4)) is assessed as a function of propagation distance in order to obtain the relative nonlinearity parameter. The wedge transducer used for generation is clamped to the sample in each measurement set, while Rayleigh waves are measured for propagation distances that vary between  $x_{min} = 30$  mm and  $x_{max} = 78$  mm with an increment of 2 mm, by moving the air-coupled transducer. It has been experimentally observed with the air-coupled transducer setup that the ultrasonic Rayleigh wave beam does not come out of the exact center of the wedge transducer, but instead has a small offset. Moreover, the actual beam does not propagate along a line perpendicular to the transducer plane. For this reason, the beam axis in the  $x - y$  plane needs to be experimentally determined a priori. This turns out to be very important for a repeatable result by minimizing misalignment errors. The nonlinear measurements are performed along this

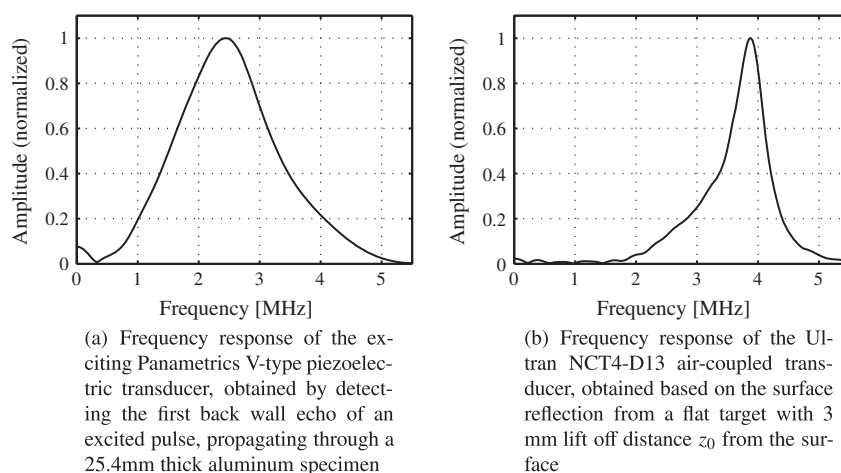
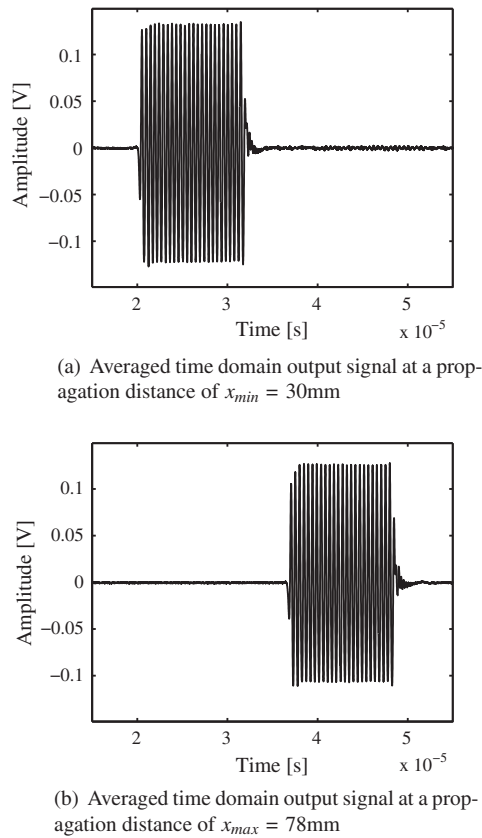
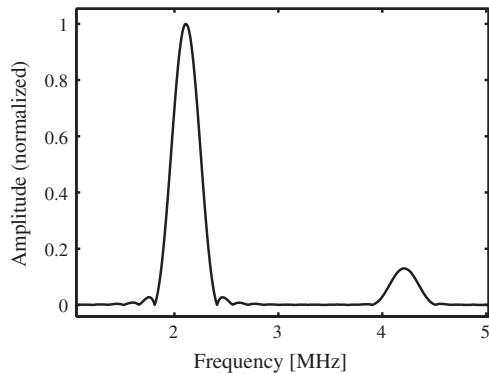


Fig. 2. Frequency response of the exciting and receiving transducer.



**Fig. 3.** Typical 256-times averaged output signals of the receiving transducer at the minimum and maximum propagation distances.



**Fig. 4.** Amplitude of the first and the second harmonics in the frequency-domain, obtained by performing a Fast Fourier transformation on the steady state portion of the time domain signal. The amplitude is normalized by the maximum amplitude of the first harmonic component.

predetermined line. The adjustment of the angle  $\Theta_R$  of the leaked longitudinal wave can be made based on the received signal from the air-coupled transducer by looking for the angle at which the received output signal has the highest amplitude for each specimen. The lift off distance,  $z_0$  between the transducer and the specimens needs to be as consistent as possible throughout all measurements to keep the attenuation and diffraction of the leaked longitudinal wave in air constant.

### 3.3. Data processing

In order to obtain the amplitudes of the fundamental and second harmonic wave components, the steady state portion of the

time-domain signal (Fig. 3) is identified and a Hann window is applied to eliminate the ringing effects of the transducer. The time-domain signal is mapped to the frequency-domain using the Fast Fourier transform (FFT). The frequency-domain signal is shown in Fig. 4, where one can clearly see the contributions of the fundamental and second harmonic waves. The amplitudes of the measured fundamental (first) and second harmonics are denoted as  $A_1^{el}$  and  $A_2^{el}$ . These values are uncalibrated electrical amplitudes, but are proportional to the absolute particle displacements in the material. So the relative acoustic nonlinearity parameter  $\beta'$ , calculated using these relative amplitude values is

$$\beta' = \frac{A_2^{el}}{(A_1^{el})^2} \propto \frac{\bar{u}_z(2\omega_0)}{\bar{u}_z^2(\omega_0)x} \propto \beta. \quad (9)$$

This relative acoustic nonlinearity parameter,  $\beta'$  will be used as a relative measure of the material nonlinearity to make comparisons between different material nonlinearities since all setup parameters will be kept constant throughout the measurements for different specimens.

## 4. Specimen preparation

An aluminum 2024-T351 plate and an aluminum 7075-T651 plate, both 25.4 mm thick are used to demonstrate the accuracy of the proposed non-contact air-coupled Rayleigh wave measurements since there are results available for comparison in the published literature. The Al 2024-T351 plate is heat treated at 325 °C for three hours and air cooled in an uncontrolled atmosphere to reduce the influence of cold work associated with the T351 tempering process. Note that the Al 7075-T651 alloy is solution heat treated and artificially aged, as indicated by T651. Both plates are hand-polished using 800 grade sandpaper to obtain the same surface conditions. The differences in material nonlinearity in aluminum alloys are caused by alloying elements, which can lead to the formation of precipitates in the lattice structure as shown by Cantrell and Yost [1]. Precipitates can either be incoherent, semi-coherent, or coherent with the lattice structure, depending on their size, but only coherent precipitates can act as pinning points for dislocations [13] and lead to the generation of a second harmonic wave component as shown by Hikata et al. [14]. Precipitation in aluminum can occur during natural aging at room temperature or during artificial aging at elevated temperatures. The aging parameters and the amount of alloying elements strongly influence the nonlinearity of the specimen since these can significantly change the amount of second phase precipitates as well as their size and distribution.

## 5. Results and discussion

Nonlinear Rayleigh surface wave measurements along the rolling direction of the Al 2024-T351 and Al 7075-T651 plates are performed with the proposed setup. The standard deviation of the linear fit to the normalized second harmonic  $A_2^{el}/(A_1^{el})^2$  over the propagation distance is calculated to be below 2% for three different sets of measurements in which the generating wedge transducer is removed and reattached for each measurement set. This shows that the measurement based on the non-contact air-coupled receiver is highly repeatable and thus the measured acoustic nonlinearity parameters,  $\beta'$  are reliable. Note that no near field effects are observed in this experimental setup, i.e. no amplitude fluctuations are observed at propagation distances longer than 30 mm (Fig. 5).

Measurements are taken along two different lines of propagation in each plate to assess the spatial variation within the specimen. The linear ultrasonic properties of the two aluminums (i.e.



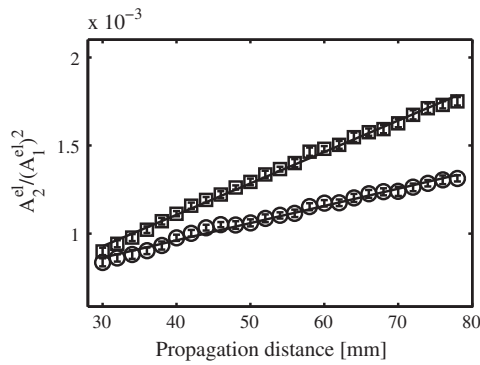


**Fig. 5.** Ratio  $A_2^{el}/(A_1^{el})^2$  obtained by three measurements with reattached exciting wedge-transducer are plotted over propagation distance for the Al 7075-T651 ( $\square$ ) and Al 2024-T351 ( $\circ$ ) specimen, note that each individual data point consists of three measurements and that the error bars are smaller than the data point symbols.

the Rayleigh wave speeds) are assumed to be identical. Representative results for the normalized second harmonic amplitude versus the propagation distance obtained from the two material specimens are shown in Fig. 5 where one can clearly see negligibly small error bars in both sets of measurements, plus the higher relative acoustic nonlinearity of Al 7075-T651 when compared to Al 2024-T351.

A relatively large spatial variation of the relative acoustic nonlinearity parameter is observed in the Al 2024-T351 sample ( $\pm 10\%$ ), while there is a negligible spatial variation in Al 7075-T651 ( $\pm 1.5\%$ ) observed. Such variations can be caused by differences in chemical composition and cooling rates which can lead to a spatially nonuniform precipitate density and microstructural features. The measured relative nonlinearity parameters  $\beta'$  of the two aluminum plates and their ratio are shown in Table 1.

To validate the result of these air-coupled measurements, consider the results presented in [15,16], which used a capacitive receiver to measure nonlinear longitudinal waves. Yost and Cantrell [15] measured the nonlinearity parameters of Al 2024 and Al 7075 specimens but did not specify the heat treatments of the samples. Li et al. [16] examined aluminum alloys to characterize the dependence of the acoustic nonlinearity parameter on second phase precipitates in Al 2024-T4 and Al 7075-T551 specimens. Note that one-to-one comparisons of the values in Table 2 are not entirely desirable since the nonlinearity of aluminum alloys is highly dependent on the chemical composition and the heat treatment of the specimen, while both references do not use specimens with the exact same treatment and chemical composition that was used in this research. However, the overall agreement shown in this table and in Fig. 6 are useful in demonstrating the accuracy of an air-coupled receiver for nonlinear Rayleigh wave measurements.

The acoustic nonlinearity parameters measured by Yost and Cantrell [15] suggest a ratio  $\beta_{7075}/\beta_{2024}$  between 2.03 and 1.70. However, earlier research on Al 2024-T4 and Al 7075-T551 by Li et al. [16] yields a ratio of 1.28–0.97. An average ratio greater than 1 is obtained in both studies, which is consistent with the results

**Table 1**  
Relative acoustic nonlinearity parameters obtained using Rayleigh surface waves with air-coupled detection and the ratio  $\beta_{7075}'/\beta_{2024}'$ , which can be used for comparison with literature data of acoustic nonlinearity parameters.

Material	$\beta' (\times 10^5)$	$\beta_{7075}'/\beta_{2024}'$
Al 7075-T651	$1.785 \pm 0.027$	1.85–1.50
Al 2024-T351	$1.074 \pm 0.097$	

**Table 2**  
Literature data of the acoustic nonlinearity parameters for Al 2024 and Al 7075 and the ratio  $\beta_{7075}/\beta_{2024}$  obtained by Yost and Cantrell [15] and Li et al. [16].

Reference	Material	$\beta$	$\beta_{7075}/\beta_{2024}$
Yost and Cantrell [15]	Al 7075	$7.6 \pm 0.34$	2.03–1.70
	Al 2024	$4.09 \pm 0.18$	
Li et al. [16]	Al 7075-T551	$8.6 \pm 0.60$	1.28–0.97
	Al 2024-T4	$7.7 \pm 0.54$	

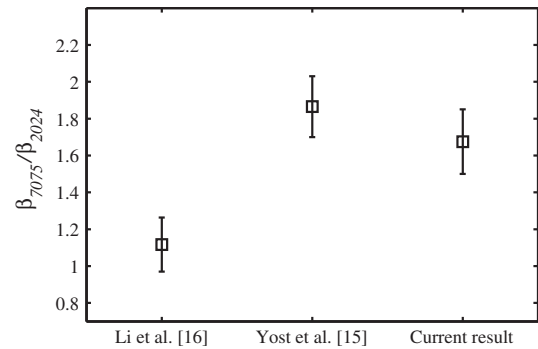


**Fig. 6.** Comparison of the ratio of the obtained nonlinearity parameters for Al 2024 and Al 7075 with literature data by Yost and Cantrell [15] and Li et al. [16].

from the current measurements where there are ratios between 1.85 and 1.50 of the relative nonlinearity parameters  $\beta_{7075}'$  and  $\beta_{2024}'$ .

## 6. Conclusions

This research demonstrates the robustness and high accuracy of using a non-contact, air-coupled receiver for the measurement of the acoustic nonlinearity parameter with Rayleigh surface waves. The experimental setup provides an output signal with sufficiently high SNR and potential experimental inconsistencies due to the coupling variability of the generating wedge transducer are shown to be negligible. An additional advantage is that the surface condition of the specimen is relatively unimportant in this measurement setup. The experimental results obtained with the proposed measurement setup are validated by comparisons with literature data. The higher relative acoustic nonlinearity of Al 7075 as compared to Al 2024 is consistent with the results of Yost and Cantrell [15] and Li et al. [16]. The results obtained in this research demonstrate that nonlinear Rayleigh surface wave measurements using air-coupled detection can accurately assess the relative acoustic nonlinearity parameter,  $\beta'$  and potentially the absolute nonlinearity parameter,  $\beta$  if calibrations and diffraction corrections are made.

## Acknowledgements

This work is supported by the German Academic Exchange Service (DAAD) through a Graduate Research Assistantship for Sebastian Thiele and is being performed using funding received from the DOE Office of Nuclear Energy's Nuclear Energy University Programs. Additional funding has been provided by the Electric Power Research Institute (EPRI).

## References

- [1] J.H. Cantrell, W.T. Yost, *J. Appl. Phys.* **81** (1997) 2957–2962.
- [2] J.S. Valluri, K. Balasubramaniam, R.V. Prakash, *Acta Mater.* **58** (2010) 2079–2090.
- [3] J.-Y. Kim, L.J. Jacobs, J. Qu, J.W. Littles, *J. Acoust. Soc. Am.* (2006) 1266–1273.

- [4] A. Ruiz, N. Ortiz, A. Medina, J.-Y. Kim, L.J. Jacobs, *NDT&E Int.* 54 (2013) 19–26.
- [5] K.H. Matlack, J.J. Wall, J.-Y. Kim, J. Qu, L.J. Jacobs, H.-W. Viehrig, *J. Appl. Phys.* 111 (2012).
- [6] S.V. Walker, J.-Y. Kim, J. Qu, L.J. Jacobs, *NDT&E Int.* 48 (2012) 10–15.
- [7] M. Liu, J.-Y. Kim, L.J. Jacobs, J. Qu, *NDT&E Int.* 44 (2011) 67–74.
- [8] D.C. Hurley, C.M. Fortunko, *Meas. Sci. Technol.* 8 (1997) 634–642.
- [9] J. Herrmann, J.-Y. Kim, L.J. Jacobs, J. Qu, J.W. Little, *J. Appl. Phys.* 99 (2006).
- [10] A. Cobb, M. Capps, C. Duffer, J. Feiger, K. Robinson, B. Hollingshaus, in: D.O. Thomson, D.E. Chimenti (Eds.), *Review of Progress in Nondestructive Evaluation*, vol. 31, Plenum Press, New York, 2012, pp. 299–306.
- [11] M.O. Deighton, A.B. Gillespie, R.B. Pike, R.D. Watkins, *Ultrasonics* (1981) 249–258.
- [12] D.J. Shull, E.E. Kim, M.F. Hamilton, E.A. Zabolotskaya, *J. Acoust. Soc. Am.* 97 (1995) 2126–2137.
- [13] J.H. Cantrell, X.-G. Zhang, *J. Appl. Phys.* 84 (1998) 5469–5472.
- [14] A. Hikata, B.B. Chick, C. Elbaum, *J. Appl. Phys.* 36 (1965) 229.
- [15] W.T. Yost, J.H. Cantrell, in: D.O. Thomson, D.E. Chimenti (Eds.), *Review of Progress Nondestructive Evaluation*, vol. 12, Plenum Press, New York, 1993, pp. 2067–2073.
- [16] P. Li, W.T. Yost, J.H. Cantrell, K. Salama, *IEEE 1985 Ultrasonics Symposium*, 1985, pp. 1113–1115.